

Anatomy of the Market: A Body–Tail Test of Factor Models

Useong Shin*

June 29, 2026

JEL: G12; G11; C52; C58

Keywords: asset pricing; factor models; body–tail test; market portfolio; test assets; pricing errors; model evaluation

Abstract

In an ideal stochastic discount factor, zero pricing errors and the maximum Sharpe ratio coincide; in a low-dimensional approximation they need not. I study this separation by decomposing an investible CRSP market portfolio into dynamic value-weighted body and tail legs that recombine to the market return. All models pass the aggregate benchmark, and the recombination identity does not require zero leg alphas. Yet the identity holds for every model, while only q5 leaves systematic offsetting leg alphas—negative in the body, positive in the tail—and falls below its market-only baseline, despite dominating on spanning. Matched random splits remove the pattern.

*Sogang Business School, Sogang University (Seoul, Korea).
ORCID: [0009-0003-0197-9003](https://orcid.org/0009-0003-0197-9003)
Email: useong@sogang.ac.kr

1 Introduction

In an ideal stochastic discount factor two criteria coincide: the SDF prices every asset with zero alpha, and the tangency portfolio it spans attains the maximum Sharpe ratio. For a low-dimensional approximation they need not. [Barillas and Shanken \(2017\)](#) make one half precise—because zero-alpha tests depend on the chosen test assets while the maximum Sharpe ratio does not, *model comparison* should rest on spanning, not on alphas over an arbitrary asset set. This paper examines the other half: a model favored on the Sharpe-ratio criterion can still leave systematic pricing errors on a particular set of test assets, and I document one such separation.

Most factor models include the market return, so passing an aggregate-market test is a natural but weak check: a value-weighted market portfolio can have a small alpha even when its components carry offsetting errors. I study this with a body–tail decomposition of an investible CRSP market portfolio, split by cumulative market capitalization. The legs are tradable portfolios whose dynamic value-weighted recombination exactly recovers the original market return, so the aggregate benchmark is held fixed and only the test asset changes. The legs need not inherit the market’s alpha—the recombination identity aggregates leg alphas back to the market alpha, so a nonzero leg alpha is not itself evidence against a model. The diagnostic content lies in the cross-model comparison: because the identity holds for *every* candidate model, any difference in the leg pattern cannot be a mechanical consequence of splitting, so the test reads that asymmetry, not the presence of leg alphas, as informative.

I compare CAPM, FF3, Carhart, FF5, FF6, and q5. After verifying that my production market return, cMKT, tracks standard market factors and passes the aggregate check, I estimate body and tail alphas across nine cumulative-market-capitalization cutoffs and run matched random splits that hold the universe, dates, split ratios, and aggregate return fixed while removing only the size-ranked assignment rule.

The aggregate tests are uneventful: every model prices the production market return with insignificant alpha, but the body–tail tests separate them. CAPM, Carhart, FF5, and FF6 are broadly stable; q5 is the exception, with a negative body alpha and positive tail alpha at all nine ratios and a daily joint rejection—sharp precisely because q5 is the strongest candidate on the spanning criterion, not the weakest. Matched random splits remove the pattern, and a battery of diagnostics—alternative HAC lags, cMKT substitution, monthly aggregation, external size deciles, factor-block ablations, and a loading–premium decomposition—traces it to q5’s nonmarket profitability–growth block rather than a market-factor implementation issue. The evidence does not replace or challenge the spanning criterion of [Barillas and Shanken \(2017\)](#); it adds a third object: aggregate market fit, mean–variance spanning, and

the alpha pattern on an economically ordered decomposition are distinct, and the body–tail design makes the third visible.

2 Theoretical Background and Related Literature

2.1 Two Criteria for Evaluating an Approximate SDF

Linear factor models summarize common return variation with a few factors and price expected returns through exposures to them. Let $R_{i,t}^e$ be the excess return on test asset i and f_t a K -vector of factor returns; the standard time-series test estimates

$$R_{i,t}^e = \alpha_i + \beta_i' f_t + \varepsilon_{i,t}, \quad i = 1, \dots, N, \quad (1)$$

where the intercept α_i is the pricing error and the GRS test of [Gibbons et al. \(1989\)](#) jointly tests $\alpha_i = 0$ across the set. The same logic follows from the stochastic discount factor (SDF) approach, in which a valid SDF prices all traded assets and a factor model is a low-dimensional approximation to it ([Cochrane, 2005](#); [Hansen and Jagannathan, 1997](#)). By [Kozak et al. \(2018\)](#), the absence of near-arbitrage lets the SDF be represented through a few *high-variance* return directions, so a low-dimensional model approximates the SDF along its dominant covariance directions and leaves pricing errors that are larger where expected-return variation is poorly aligned with those directions. Evaluation therefore concerns not only which anomalies a model explains but which pricing errors it leaves on a given asset set.

For an *ideal* SDF these distinctions vanish—the SDF that prices every asset is spanned by the maximum-Sharpe-ratio tangency portfolio—but for an approximation they come apart. [Barillas and Shanken \(2017\)](#) make one side precise: for traded-factor models, comparing one against another reduces to whether each prices the other’s factors, so common test-asset alphas add nothing and *test assets are irrelevant for model comparison*, leaving factor spanning—linked to the maximum Sharpe ratio—as the criterion; [Barillas and Shanken \(2018\)](#) develop the same mean–variance comparison. I take this as given. The body–tail exercise does not compare models by their alphas and is no substitute for spanning; it examines the other side of the gap—whether a model *avored* on spanning still leaves systematic pricing errors on a particular, economically ordered set of test assets derived from the market it already prices.

2.2 Aggregate Market Alpha and Decomposition Diagnostics

Because every model here contains a market factor, a small alpha for the aggregate market portfolio is a sanity check rather than strong evidence about pricing elsewhere, especially when the market portfolio is measured from data close to the factor itself. It also does not mechanically imply small alphas on subsets of the same universe. In a fixed-weight case, let the market M combine two tradable legs B and T :

$$R_{M,t}^e = w_B R_{B,t}^e + w_T R_{T,t}^e, \quad w_B + w_T = 1. \quad (2)$$

Under the same model the market alpha is the weighted average of the leg alphas,

$$\alpha_M = w_B \alpha_B + w_T \alpha_T, \quad (3)$$

so $\alpha_M = 0$ does not imply $\alpha_B = \alpha_T = 0$: a nonzero leg alpha is not itself evidence against a model, and offsetting leg errors are consistent with a small aggregate alpha. The diagnostic content lies in the comparison. Equation (3) is an accounting identity that holds for *every* model regardless of f_t , so any *cross-model difference* in the leg pattern cannot be a mechanical consequence of the split. The test reads that asymmetry, not the presence of leg alphas, as informative; the leg weights vary over time in the buy-and-hold setting, but the same logic applies to the dynamic reconstruction below. This is also why the exercise does not conflict with test-asset irrelevance, which concerns model *comparison*: the body–tail design asks, for one model at a time, whether it prices a size-ranked decomposition of the market it already prices in aggregate—internal pricing consistency, not mean–variance dominance.

2.3 Test-Asset Construction and the Position of This Paper

Empirical performance can depend on how test assets are constructed: when test assets and candidate factors share sorting rules, good fit can reflect both general pricing ability and alignment with the test-asset design. [Lo and MacKinlay \(1990\)](#) raise data-snooping concerns, [Lewellen et al. \(2010\)](#) show inference is sensitive to test-portfolio structure, and [Giglio et al. \(2025\)](#) stress the joint role of test assets and weak factors—the slack an approximate SDF leaves open, since by [Kozak et al. \(2018\)](#) different test assets weight different directions of misspecification. Body–tail legs are not anomaly portfolios sorted on book-to-market, profitability, investment, or momentum; they are size-ranked portfolios from the same investible universe whose value-weighted combination reconstructs the aggregate market return, fixing the benchmark they recombine to. A companion study ([Shin, 2026](#)) documents related construction dependence using CRSP-based random portfolios not presorted on characteristics;

here the test assets are tied by construction to a market portfolio the models already price. I also use random splits, which hold everything fixed but assign stocks at random rather than by market-capitalization rank, as placebo benchmarks that separate the size-ranked rule from the act of forming two legs.

I compare standard models for U.S. equity returns. The Fama–French three-factor model includes market, size, and value (Fama and French, 1993); the five-factor model adds profitability and investment (Fama and French, 2015); Fama and French (2018) discuss factor selection; and the Carhart model adds momentum (Jegadeesh and Titman, 1993; Carhart, 1997). The q-factor family is based on investment-based asset pricing: Hou et al. (2015) propose market, size, investment, and profitability factors, Hou et al. (2019) weigh competing factors, and Hou et al. (2021) add an expected-growth factor to form q5, with Hou et al. (2020) on anomaly replication and Hou et al. (2024) on security-analysis information. On the spanning criterion these models are strong—as the tests below confirm, q5’s profitability and expected-growth factors expand the mean–variance frontier well beyond the Fama–French factors, which makes q5 the informative case rather than a weak-model counterexample. The goal is not to name a single best model; a model can expand the opportunity set and still leave alphas on a specified set of portfolios. I therefore evaluate alphas on a body–tail decomposition rather than only on characteristic-sorted portfolios, benchmark them against matched random splits, and use cMKT substitutions and factor-block diagnostics to locate whether the pattern stems from market-factor implementation or a nonmarket block.

3 Data and Methodology

3.1 CRSP Universe Selection

I build an investible U.S. equity universe from daily CRSP data over January 3, 1967 to December 31, 2024. The base sample is NYSE, AMEX, and NASDAQ common stocks; the screen keeps almost all of the market’s economic scale and trading activity while excluding the extreme microcap and illiquidity tails.

Investibility is updated each month-end using both market capitalization and liquidity. For stock i , month-end market capitalization is

$$ME_{i,t} = |PRC_{i,t}| \times SHROUT_{i,t} \times 1,000, \quad (4)$$

and its cumulative market-capitalization share, after sorting in descending order of ME , is

$$CumME_{i,t} = \frac{\sum_{j:ME_{j,t} \geq ME_{i,t}} ME_{j,t}}{\sum_j ME_{j,t}}. \quad (5)$$

I measure liquidity by average dollar volume over the most recent 63 trading days ending at the month-end:

$$DVOL_{i,d} = |PRC_{i,d}| \times VOL_{i,d}, \quad (6)$$

$$ADV63_{i,t} = \frac{1}{N_{i,t}} \sum_{d \in \mathcal{W}_t} DVOL_{i,d}, \quad (7)$$

where \mathcal{W}_t is the 63-day window ending at month-end t and $N_{i,t}$ the number of its days with observed volume. I use monthly cross-sectional percentiles of $ADV63$ rather than an absolute cutoff, avoiding a fixed nominal threshold over a long sample with large changes in prices and market size.

The selection rule uses hysteresis: an incumbent exits if $CumME_{i,t} > 0.999$ or its $ADV63$ falls to the bottom 2.5% of the monthly cross-section, while an outside stock enters only if $CumME_{i,t} \leq 0.995$ and its $ADV63$ reaches at least the fifth percentile, the stricter entry rule reducing churn near the boundary. Because historical NASDAQ volume is limited early on, I defer the liquidity screen for a NASDAQ stock until 63 trading days of volume history exist, while still applying the market-capitalization screen. All screening variables use only information observed by the relevant month-end, and the universe set at a month-end applies from the first trading day of the next month, preventing look-ahead bias.

Across the full sample the final universe averages 77.6% of the common-stock base sample while preserving about 99.7% of total market capitalization and 63-day average dollar volume. At the end of December 2024 it includes 2,426 of 3,804 base-sample stocks, with market-capitalization and dollar-volume preservation rates of 99.78% and 99.28%—removing the extreme illiquidity tail while retaining almost all of the market’s economic weight.

3.2 Market-Factor Replication

The tests start from an investible market portfolio built directly from CRSP individual stocks, so I first check whether later alpha estimates could be driven by market-return implementation differences. I construct a daily value-weighted market return, $cMKT$, from the universe above; it is both the benchmark the body–tail and random-split portfolios reconstruct and the series used to gauge implementation gaps relative to standard market factors. Replicating a broad market return is not merely value-weighting all stocks: delisting

and dividend-inclusive returns, formation dates, coverage, and the treatment of small or illiquid stocks introduce small daily differences that can accumulate over decades and affect intercepts. I therefore compute $cMKT$ as a daily value-weighted buy-and-hold portfolio with the universe fixed at each month-end and applied from the next month’s first trading day, formation-date market-capitalization weights, dividend-inclusive returns, delisting returns where observed, and within-portfolio cash flows reinvested proportionally into survivors. The aim is not to reverse-engineer any provider’s factor but to ask whether an independent CRSP market return is close enough to the Fama–French and q5 factors for the decomposition tests to be meaningful.

It is. Over the common sample the correlation between $cMKT$ and the Fama–French market return is 0.999778 ($R^2 = 0.999556$), with daily RMSE 2.21 bp and mean absolute error 1.35 bp; against the q5 market return the correlation is 0.999799 ($R^2 = 0.999598$), with RMSE 2.10 bp and mean absolute error 1.27 bp. In both the beta is very close to one and the intercept economically small. The q5 factors used throughout are the daily series the providers distribute ([Global-q.org](https://global-q.org), 2026), not a frequency conversion of mine, so the daily frequency I test is one they themselves publish. Figure 3.1 shows most observations near the 45-degree line.

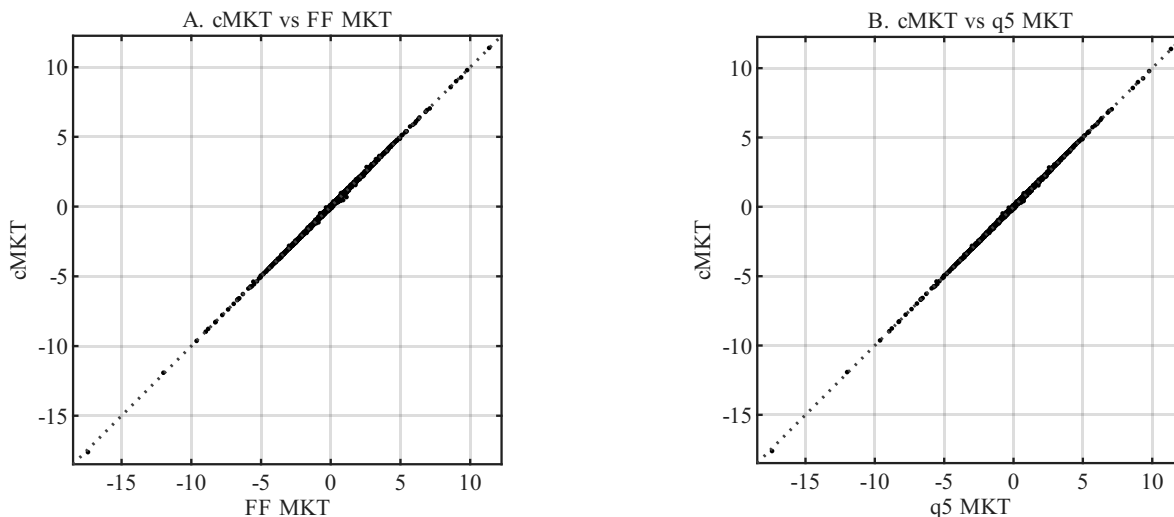


Figure 3.1: CRSP-based market return and standard market factors

Note: The figure reports daily scatter plots of $cMKT$, the market return that I construct from the CRSP investible universe, against the Fama–French and q5 market returns. The comparison uses total market returns after adding each provider’s risk-free rate back to the excess market return. The dashed line is the 45-degree line. The common sample runs from January 3, 1967 to December 31, 2024.

High accuracy does not make construction trivial—long-run alpha tests stay sensitive to delisting treatment, reinvestment, formation dates, coverage, and illiquid-stock inclusion—so

I treat the *cMKT* comparison as a diagnostic separating implementation-gap alphas from those in the test portfolios. As a sanity check, since each model contains a market factor, the intercept should be near zero when the full market portfolio is the test asset: Table 3.1 regresses the full investible market return on each model, and all have R^2 above 0.999 with every alpha p -value above 0.05 under a 21-day Newey–West lag. Unless stated otherwise, main tests use a 21-day lag and robustness checks lags of 5, 63, and 252.

Table 3.1: Market sanity check for the full market return

Model	Observations	Annual alpha (bp)	$t(\alpha)$	$p(\alpha)$	R^2
CAPM	14,598	-1.02	-0.22	0.829	0.999556
FF3	14,598	0.21	0.05	0.963	0.999571
Carhart	14,598	-0.06	-0.01	0.989	0.999571
FF5	14,598	-1.07	-0.24	0.812	0.999572
FF6	14,598	-1.18	-0.26	0.792	0.999572
q5	14,598	-5.78	-1.44	0.151	0.999619

Note: The table reports regressions of the full investible market return constructed in this paper on each candidate factor model. Alpha is the daily intercept multiplied by 252 and reported in basis points per year. All tests use the common sample from January 3, 1967 to December 31, 2024. The p -values use a Newey–West lag of 21 trading days.

The pass is a consistency gate, not a claim that implementation is irrelevant or that any portfolio from the same universe must have zero alpha: it shows only that the aggregate market is close to priced by all models under the baseline test, so later leg-level patterns are read as properties of the body–tail and random-split portfolios rather than failures of the aggregate benchmark. Nor does *cMKT* claim to replicate either provider’s factor exactly—universes, filters, and return treatments differ—only to be empirically close to both, which makes simple implementation error an unlikely standalone explanation for the body–tail results. As a more direct control, I also replace each provider’s market factor with *cMKT* to ask whether the results survive the same CRSP-based market return that generates the test portfolios.

3.3 Body–Tail Test

The core test decomposes the full market portfolio into a body and a tail—tradable test portfolios from the same investible universe as the aggregate market, yet distinct from it—so the reconstruction identity below does not impose zero alpha on each leg when the aggregate alpha is small, but provides a controlled way to examine how pricing errors distribute across a size-ranked decomposition. At each formation date τ I sort investible stocks by market

capitalization in descending order, defining the body as the stocks with cumulative share at or below the split ratio p and the tail as the remainder, with

$$p \in \{0.50, 0.60, 0.75, 0.80, 0.85, 0.90, 0.95, 0.975, 0.99\}.$$

The grid spans balanced splits and cases that isolate a small market-capitalization tail. Portfolios form at the end of each June from the universe and ranks observed then, and the split applies from the first trading day of July through the next June—close to standard Fama–French timing and insulated from high-frequency noise in the split boundary. Leg returns are value-weighted buy-and-hold returns with formation-date weights; dividend and delisting returns are treated as in the full market return, and within-leg cash flows reinvested proportionally into survivors. Because the legs are annual buy-and-hold portfolios while the factors are reconstructed at their providers’ frequencies, a leg can drift from its formation weights within the year; but any alpha from this mismatch is shared by the matched random split in Section 3.4, which uses the identical schedule, holding rule, and reinvestment accounting, so the random split absorbs such drift and a body–tail pattern it does not reproduce cannot be attributed to drift.

Let $w_{p,\tau}^B$ and $w_{p,\tau}^T$ be the initial body and tail market-value shares, with $w_{p,\tau}^B + w_{p,\tau}^T = 1$. During the holding period the shares vary with realized returns and reinvested cash flows, so the daily reconstruction identity uses previous-day-end shares:

$$R_{M,d}^e = w_{p,d-1}^B R_{B,p,d}^e + w_{p,d-1}^T R_{T,p,d}^e, \quad w_{p,d-1}^B + w_{p,d-1}^T = 1,$$

where $R_{M,d}^e$ is the full investible market excess return and $R_{B,p,d}^e$, $R_{T,p,d}^e$ the leg excess returns. The identity makes the legs reconstruct the same aggregate market return without making them equivalent to it as test assets.

I estimate leg pricing errors with standard time-series regressions,

$$R_{\ell,p,d}^e = \alpha_{\ell,p} + \beta'_{\ell,p} f_d + \varepsilon_{\ell,p,d}, \quad \ell \in \{B, T\},$$

where f_d is the daily factor vector. I test each leg alpha separately and the joint restriction $H_0 : \alpha_{B,p} = \alpha_{T,p} = 0$ with a Wald test using the between-leg residual covariance and Newey–West matrices (baseline lag 21 trading days). Because the nine ratios are nested cuts of the same universe their tests are not independent; I read rejection counts as within-model robustness and base cross-model statements on the contrast at the identical grid. I also estimate the recombined net-portfolio alpha and verify the identity numerically, confirming that a small, insignificant aggregate alpha does not mechanically determine the leg alphas.

3.4 Random Split Test

Random splits test whether the body–tail results are specific to size-ranked assignment rather than to the act of splitting. They use the same universe, formation dates, holding periods, split ratios, accounting, models, and statistics as the body–tail test; only the assignment rule changes, with stocks assigned to two groups at random at each formation date. Each split is matched to a body–tail ratio, so at $p = 0.80$ one leg holds about 80% of market value and the other 20%, giving both tests the same aggregate portfolio and similar leg shares. Specifically, at τ I randomly permute the investible stocks and assign them to the random A-leg until cumulative capitalization reaches p , the remainder forming the B-leg; each pair satisfies the same reconstruction identity using previous-day-end shares:

$$R_{M,d}^e = w_{p,d-1}^A R_{A,p,d}^e + w_{p,d-1}^B R_{B,p,d}^e, \quad w_{p,d-1}^A + w_{p,d-1}^B = 1.$$

The random split is not a structural simulation under the null that a model is true; it is a placebo benchmark for the split procedure, showing what alphas arise simply from dividing the market into two value-weighted legs with similar shares—which matters because the smaller leg has higher volatility and less precise alphas as p rises. The contrast is the main evidence: similar leg alphas and rejection frequencies in both designs would indict splitting itself, whereas small or directionless random splits alongside systematic body–tail rejections point to the size-ranked rule. I treat it as a matched placebo, not a secondary robustness check.

4 Spanning Tests Across Factor Models

Before the body–tail test, I examine mean–variance inclusion relations among the traded factor models. As Section 2.1 notes, [Barillas and Shanken \(2017\)](#) establish that for traded models the comparison of one against another is governed by factor spanning and linked to the maximum Sharpe ratio, so common test-asset alphas do not determine the ranking. Running the spanning tests first fixes which model is favored on that criterion, so any later body–tail evidence is read against that baseline rather than as a generic weakness. The two analyses answer different questions: a model that leaves significant body–tail alphas is not thereby inferior in the mean–variance sense, and a larger opportunity set need not imply pricing of the market’s internal components.

4.1 Test Design

FF6 consists of the market, size, value, profitability, investment, and momentum factors; q5 of the market, size, investment, return-on-equity, and expected-growth factors. Portfolio pricing tests use each provider’s market factor and risk-free rate, but the mutual spanning tests use a common market factor, to avoid placing two nearly identical market factors on opposite sides of the same regression. Baseline results use the Fama–French market factor; I confirm them with the global-q market factor. I define the nonmarket blocks as

$$g_t^q = (ME_t, IA_t, ROE_t, EG_t)',$$

$$g_t^{FF} = (SMB_t, HML_t, RMW_t, CMA_t, MOM_t)',$$

and estimate the mutual spanning regressions

$$g_t^q = \alpha_{q|FF6} + B_{q|FF6} f_t^{FF6} + \mathbf{u}_{q,t}, \quad (8)$$

$$g_t^{FF} = \alpha_{FF|q5} + B_{FF|q5} f_t^{q5} + \mathbf{u}_{FF,t}, \quad (9)$$

with nulls $H_0 : \alpha_{q|FF6} = \mathbf{0}$ and $H_0 : \alpha_{FF|q5} = \mathbf{0}$. I test the joint intercepts with the GRS test and a HAC Wald test (Newey–West lag 21 trading days for daily data, 6 months for monthly). The common daily sample is January 3, 1967 to December 31, 2024 (14,598 observations); the monthly sample, from compounding daily returns within calendar months, has 696. I measure the excluded block’s economic contribution by

$$\Delta \text{SR}^2 = \hat{\alpha}' \hat{\Sigma}_u^{-1} \hat{\alpha}, \quad (10)$$

the annualized increase in the squared maximum Sharpe ratio; the spanning decision itself rests on the joint intercept tests.

4.2 Joint and Factor-Level Spanning Results

Table 4.1 reports the joint results. In daily data both nulls are strongly rejected—neither model fully absorbs the other’s nonmarket factors—but the magnitudes are asymmetric: adding the q5 block to FF6 raises the annualized maximum Sharpe ratio from 1.311 to 2.205 ($\Delta \text{SR}^2 = 3.143$), whereas adding the FF6 block to q5 raises it from 2.077 to 2.205 ($\Delta \text{SR}^2 = 0.549$).

The monthly results agree in one direction: the null that FF6 spans q5 is strongly rejected, while in the reverse direction the GRS and HAC p -values straddle the 5% level (0.051 and 0.044), so the decision depends on the inference method. The global-q market factor leaves

this unchanged. Monthly data thus suggest q5 absorbs much of the FF6 block but do not support robust complete spanning. The baseline for the body–tail tests is therefore clear: on the spanning and maximum–Sharpe–ratio criterion q5 has strong evidence in its favor, so if q5 later leaves significant leg–level alphas, the finding cannot be reduced to q5 being a generally weak model. The same model can look strong by mean–variance spanning and fragile by aggregation consistency inside the market portfolio.

Table 4.1: Joint Spanning Tests Across Factor Models and Maximum Sharpe Ratios

Frequency	Null hypothesis	GRS	GRS p	HAC Wald	HAC p	SR ₀	Δ SR ²
Daily	FF6 \supseteq q5	45.197	< 0.001	148.177	< 0.001	1.311	3.143
Daily	q5 \supseteq FF6	6.248	< 0.001	23.086	< 0.001	2.077	0.549
Monthly	FF6 \supseteq q5	34.500	< 0.001	114.540	< 0.001	1.222	2.687
Monthly	q5 \supseteq FF6	2.217	0.051	11.426	0.044	1.982	0.255

Notes: $FF6 \supseteq q5$ is the null that FF6 jointly spans the q5-specific factors ME, IA, ROE, and EG. $q5 \supseteq FF6$ is the null that q5 jointly spans the FF6-specific factors SMB, HML, RMW, CMA, and MOM. SR₀ is the annualized sample maximum Sharpe ratio of the benchmark model. Δ SR² is the annualized increase in the squared maximum Sharpe ratio from adding the other model’s factor block. The reported results use the Fama–French market factor as the common market factor. The spanning decisions are unchanged when I use the global-q market factor. The HAC lag is 21 for daily data and 6 for monthly data.

Table 4.2 locates the asymmetry. FF6 almost fully absorbs ME and renders IA insignificant at 5%, but ROE and EG leave significant annualized alphas of 313.6 and 864.4 bp; EG alone has an individual Δ SR² of 2.425, the single largest source of the q5 block’s expansion of the FF6 opportunity set. In the reverse direction q5 largely absorbs HML, RMW, CMA, and MOM, leaving only SMB significant (92.3 bp), which drives the borderline monthly joint test. Because the joint statistic uses the residual covariance matrix, individual Δ SR² values should not be summed.

Table 4.2: Monthly Factor-Level Spanning Regressions

Benchmark model	Target factor	Annualized alpha (bp)	HAC p	R^2	Individual ΔSR^2
<i>Panel A: Pricing q5-specific factors with FF6</i>					
FF6	ME	17.6	0.605	0.950	0.005
FF6	IA	74.6	0.070	0.855	0.074
FF6	ROE	313.6	< 0.001	0.642	0.347
FF6	EG	864.4	< 0.001	0.449	2.425
<i>Panel B: Pricing FF6-specific factors with q5</i>					
q5	SMB	92.3	0.006	0.956	0.170
q5	HML	119.8	0.348	0.485	0.025
q5	RMW	13.3	0.895	0.473	0.001
q5	CMA	-13.7	0.755	0.861	0.003
q5	MOM	-42.0	0.843	0.277	0.001

Notes: The sample covers 696 months from January 1967 to December 2024. Alphas are monthly intercepts multiplied by 12 and reported in basis points. HAC p -values use a Newey–West lag of 6 months. Individual ΔSR^2 is the annualized increase in the squared maximum Sharpe ratio from adding each target factor alone to the benchmark model.

In sum, the spanning tests give q5 a favorable baseline: ROE and EG expand the opportunity set beyond FF6 by economically large amounts, and in monthly data q5 absorbs much of the FF6 block. The body–tail evidence below should therefore not be read as q5 being inferior in the mean–variance sense. The narrower point is the one the paper develops—a model can be strong on the criterion of [Barillas and Shanken \(2017\)](#) and still leave systematic alphas on a size-ranked decomposition of the market it prices—and it is worth flagging which factors carry that tension: the same ROE and expected-growth block that drives q5’s advantage here, with EG alone accounting for $\Delta SR^2 = 2.425$, is the block that [Section 7](#) traces the body–tail pattern to. The factors that most expand the opportunity set are thus the ones most associated with the leg-level errors—exactly the separation between the two criteria that an approximate SDF permits.

5 Full–Period Empirical Results

The market-level sanity check shows the production market portfolio is closely explained by all candidate models, so the tests below do not begin from an aggregate return the models already fail to price. They ask a narrower question: whether additional alpha patterns appear when the same investible universe is organized into size-ranked body and tail portfolios, and whether those patterns differ across models that all pass the aggregate benchmark.

5.1 Body–Tail Test

Table 5.1 summarizes the full-period tests. For each split ratio p , the body holds the top p share of cumulative market capitalization at formation and the tail holds the rest; for each pair I test the joint zero-alpha null with a Wald test.

The models separate cleanly on the identical grid. CAPM, Carhart, FF5, and FF6 do not reject the joint null at any ratio under the baseline HAC lag, and FF3 rejects at four ratios but not the net-alpha test. q5 stands apart: it rejects at all nine ratios, with a negative average body alpha and a positive average tail alpha. As noted in Section 3.3, the nine ratios are nested cuts of the same universe, so the counts describe within-model robustness rather than nine independent rejections. The informative quantity is the cross-model contrast: under the same identity, universe, and statistic, only q5 produces a systematic opposite-signed leg pattern, and the aggregate benchmark that all six models pass does not reveal it.

Table 5.1: Full-period body–tail tests

Model	Joint reject (/9)	Alpha-sum reject (/9)	Net reject (/9)	Body α (bp/yr)	Tail α (bp/yr)	Median joint p
CAPM	0/9	0/9	0/9	-18.3	82.3	0.775
FF3	4/9	4/9	0/9	18.5	-101.6	0.212
Carhart	0/9	0/9	0/9	7.0	-32.0	0.612
FF5	0/9	0/9	0/9	-3.1	-13.6	0.721
FF6	0/9	0/9	0/9	-10.7	36.2	0.588
q5	9/9	8/9	0/9	-56.2	181.0	6.25×10^{-5}

Notes: The table summarizes body–tail pair tests across nine split ratios, $p \in \{0.50, 0.60, 0.75, 0.80, 0.85, 0.90, 0.95, 0.975, 0.99\}$. The sample is the common daily sample, 1967–2024, with Newey–West 21 daily lags. “Joint reject” counts rejections of the two-leg zero-alpha Wald test at the 5% level. “Alpha-sum reject” counts rejections for the unweighted sum of the two leg alphas. “Net reject” counts rejections for the value-weighted net market portfolio reconstructed from the two legs. Because the nine ratios are nested, the counts describe within-model robustness, not independent tests.

Table 5.2 reports q5 by split ratio. The body alpha is negative and the tail alpha positive at every ratio, with the tail alpha positive even when the tail is small, so the sign pattern is not produced by one cutoff but holds across the full grid.

Table 5.2: q5 body–tail alphas by split ratio

Split p	Body α (bp/yr)	Tail α (bp/yr)	t_A	t_B	Joint p	$\alpha_A + \alpha_B$ (bp/yr)	Sum p
0.500	-158.4	147.9	-4.54	4.37	3.30×10^{-5}	-10.5	0.191
0.600	-119.4	165.4	-4.60	4.47	2.57×10^{-5}	45.9	7.40×10^{-4}
0.750	-74.6	201.1	-5.01	5.00	2.40×10^{-6}	126.5	2.47×10^{-6}
0.800	-59.1	207.8	-5.03	5.14	1.21×10^{-6}	148.7	8.36×10^{-7}
0.850	-38.0	177.1	-4.17	4.29	6.25×10^{-5}	139.1	3.82×10^{-5}
0.900	-23.8	156.5	-3.37	3.53	0.001	132.7	6.75×10^{-4}
0.950	-14.4	159.1	-2.71	2.94	0.007	144.6	0.005
0.975	-9.8	152.0	-2.11	2.23	0.040	142.2	0.031
0.990	-8.5	262.0	-1.98	2.90	0.009	253.5	0.004

Notes: This table reports the q5 body–tail results for each split ratio in the common daily sample with Newey–West 21 daily lags. A denotes the body leg and B denotes the tail leg. Alphas are annualized basis points. The net reconstructed market alpha is -5.8 bp per year with $p = 0.151$ for every split ratio because the two legs reconstruct the same production market return.

The leg pattern is invisible in the aggregate benchmark: recombining the legs with their value weights recovers the production market portfolio, and the net alpha is insignificant for all models, including q5 (Table 5.2, net $\alpha = -5.8$ bp, $p = 0.151$). This is not a contradiction but the content of the diagnostic—the recombination identity holds for every model, so it cannot by itself produce a leg pattern in one model and not others. The q5 result is thus a decomposition-specific pattern across size-ranked components, not a failure to price the aggregate and not a mechanical consequence of the split that all models share.

5.2 Random Split as a Matched Placebo-Style Benchmark

The body–tail design holds the identity fixed but cannot, by itself, separate the size-ranked assignment rule from the act of splitting; the random split does. As described in Section 3.4, it shares the universe, split ratios, aggregate market portfolio, leg weights, sample, model, statistic, formation schedule, holding rule, and reinvestment accounting with the body–tail test, so any buy-and-hold drift is common to both and only the assignment rule changes. Because the tail leg shrinks as p rises, its volatility and alpha estimation error rise mechanically; matching random splits at the same ratio controls for these size, estimation, and drift effects, leaving the assignment rule as the sole difference. The interpretation is direct: similar leg alphas and rejection frequencies in both designs would indict the split procedure itself, whereas weak, directionless random splits alongside systematic body–tail rejections point to the size-ranked rule.

Table 5.3 makes the comparison. For q5 the random-split joint rejection rate is 4.1%,

near the nominal 5%: split the same market at the same ratios without size ranking and the q5 pattern collapses to noise, while with size ranking it rejects at all nine ratios. The full-period q5 result is therefore not a split effect but is concentrated in the size-ordered decomposition. The table shows a second sense in which this is specific to q5: the Fama–French models, which do not reject the deterministic test, have random-split rates well above nominal (12.6% to 15.6% for FF5 and FF6), so the deterministic size ranking is *stabilizing* for them yet *destabilizing* for q5.

Table 5.3: Body–tail tests versus random-split benchmarks

Model	BT joint reject (/9)	Random joint reject (%)	BT sum reject (/9)	Random sum reject (%)	BT net reject (/9)	Random net reject (%)
CAPM	0/9	2.3	0/9	5.3	0/9	0.0
FF3	4/9	13.2	4/9	18.0	0/9	0.0
Carhart	0/9	8.6	0/9	13.2	0/9	0.0
FF5	0/9	15.6	0/9	20.0	0/9	0.0
FF6	0/9	12.6	0/9	17.3	0/9	0.0
q5	9/9	4.1	8/9	5.1	0/9	0.0

Notes: “BT” denotes the deterministic body–tail split. Random-split rejection rates are weighted averages across the same nine split ratios, with 500 random pairs per ratio and model. All tests use the common daily sample and Newey–West 21 daily lags. The random split preserves the same investible universe, split ratio, net market portfolio, factor model, sample period, and test statistic; only the size-ranked assignment rule is removed.

Table 5.4 gives the same comparison by ratio. The body–tail joint test rejects at every ratio while the matched random-split rate stays low throughout; even at $p = 0.99$, where the tail is very small, the random rate is only 8.2%, so the q5 result is not produced mechanically by a small tail leg but is concentrated in the size-ranked tail. The random-split alpha magnitudes rise smoothly with the ratio ($|\alpha_B|$ from 19.1 to 152.5 bp), tracing the estimation-noise channel the placebo captures, and the deterministic q5 tail alphas in Table 5.2 sit far outside that band.

Table 5.4: Matched random-split benchmark for q5

Split p	BT joint p	Random joint reject (%)	Random sum reject (%)	Random $ \alpha_A $ (bp/yr)	Random $ \alpha_B $ (bp/yr)
0.500	3.30×10^{-5}	3.0	0.0	18.9	19.1
0.600	2.57×10^{-5}	1.4	2.0	15.4	22.3
0.750	2.40×10^{-6}	2.8	3.8	10.7	30.2
0.800	1.21×10^{-6}	3.4	4.6	9.9	36.8
0.850	6.25×10^{-5}	2.8	5.0	8.9	43.3
0.900	0.001	3.8	5.8	7.6	52.9
0.950	0.007	5.4	8.0	6.6	77.0
0.975	0.040	6.0	7.8	6.1	104.9
0.990	0.009	8.2	8.6	5.8	152.5

Notes: For each split ratio, the table compares the deterministic q5 body–tail joint-test p -value with the empirical rejection rate from 500 matched random splits. All tests use Newey–West 21 daily lags. Random-split alpha magnitudes are mean absolute annualized alphas across the 500 random pairs.

6 Subperiod Empirical Results

I next examine whether the full-period evidence is concentrated in part of the sample, repeating the tests in calendar subperiods, rolling 10-year windows, and q5-detected regimes. Unless stated otherwise, all tests use the common daily sample and Newey–West standard errors with 21 trading-day lags.

6.1 Calendar subperiods

Table 6.1 reports, for each model and calendar period, how many of the nine cutoffs reject the joint zero-alpha null at 5%. The 1960s row begins in January 1967 and the 2020s row ends in December 2024.

Table 6.1: Calendar subperiod body–tail rejections

Period	Obs.	CAPM	FF3	Carhart	FF5	FF6	q5
1967–1969	727	0/9	0/9	0/9	0/9	1/9	4/9
1970–1979	2,526	0/9	0/9	0/9	0/9	0/9	2/9
1980–1989	2,528	0/9	3/9	2/9	5/9	5/9	9/9
1990–1999	2,528	0/9	4/9	0/9	0/9	0/9	0/9
2000–2009	2,515	4/9	0/9	1/9	2/9	3/9	4/9
2010–2019	2,516	0/9	0/9	0/9	0/9	0/9	0/9
2020–2024	1,258	0/9	3/9	3/9	0/9	0/9	0/9

Notes: Each entry reports the number of rejected joint zero-alpha tests among the nine body–tail split ratios. The sample is the common daily sample. HAC standard errors use 21 daily lags. Bold entries highlight q5 rejections.

Two facts emerge. First, rejection is not uniform over time: q5 rejects at all cutoffs in the 1980s but at none in the 1990s, the 2010s, or 2020–2024. Second, other models reject in some periods, yet q5 has the highest average frequency—30.2% of the joint tests across the seven subperiods, against 6.3% to 15.9% for the others. The full-period q5 result is thus not driven by one period, though it is clearly time-varying. The episodes where other models reject are themselves informative: CAPM rejects at four cutoffs only in 2000–2009, the expected behavior of a model with no size factor when the size-ranked decomposition is hardest to price. The q5 pattern is different in kind, because q5 contains size, investment, profitability, and expected-growth factors and still rejects—which is why the rest of the paper locates it in the nonmarket block rather than a missing size premium.

6.2 Rolling 10-year windows

Calendar boundaries are arbitrary, so I repeat the test in rolling 10-year windows, which reduce short-window noise and identify persistent episodes. Table 6.2 summarizes 600 windows with at least 2,000 common-sample daily observations.

Table 6.2: Rolling 10-year body–tail rejections

Model	Windows	Mean reject (%)	Median reject (%)	Any reject (%)
CAPM	600	8.1	0.0	15.0
FF3	600	14.4	0.0	38.3
Carhart	600	9.4	0.0	27.8
FF5	600	13.6	0.0	29.0
FF6	600	14.1	0.0	30.2
q5	600	40.1	44.4	79.0

Notes: The table summarizes 10-year rolling windows with at least 2,000 common-sample daily observations. Mean and median rejection shares are computed across the nine body–tail split ratios within each window. “Any rejection” is the share of rolling windows in which at least one split ratio rejects joint zero alpha at the 5% level. HAC standard errors use 21 daily lags.

The rolling windows sharpen the gap. q5 rejects 40.1% of cutoffs on average, with a median of 44.4%, and at least one cutoff rejects in 79.0% of windows; the other five models cluster between 8.1% and 14.4% on the mean with a median of 0.0%. Across 600 overlapping windows q5 is persistently the most-rejected model, by a wide margin, so the separation is not an artifact of one full-period statistic.

Table 6.3 groups the q5 windows by ending decade. Rejection is strongest in windows ending in the 1980s and 1990s, weakens through the 2000s and 2010s, and nearly vanishes in the 2020s. This time profile is itself a testable implication: a mechanical or microstructure artifact of the split would not switch on and off with the sample period, whereas a pattern driven by a specific factor block should track the periods in which that block prices strongly. Section 7 shows the block is q5’s profitability–growth side and that the decline lines up directionally with the weakening ROE and expected-growth premia, so the time variation is consistent with the mechanism the next section identifies rather than a generic artifact.

Table 6.3: q5 rolling 10-year rejections by ending decade

Ending decade	Windows	Mean reject (%)	Median reject (%)	Any reject (%)
1970s	60	24.3	22.2	93.3
1980s	120	57.4	66.7	84.2
1990s	120	61.5	66.7	99.2
2000s	120	38.2	44.4	87.5
2010s	120	30.3	22.2	70.8
2020s	60	2.0	0.0	13.3

Notes: The table groups q5 rolling 10-year windows by the decade in which the rolling window ends. Rejection shares are computed across the nine body–tail split ratios. HAC standard errors use 21 daily lags.

6.3 Detected q5 regimes

I finally use the q5 rolling rejection signal to separate periods in which q5 body–tail rejections concentrate from periods in which they are absent. The split is diagnostic—a descriptive chronology, not an out-of-sample test or a formal structural-break procedure.

Table 6.4: Detected q5 regimes and model-level rejections

Detected regime	Obs.	CAPM	FF3	Carhart	FF5	FF6	q5
Nonreject 1967–1976	2,221	0/9	0/9	0/9	0/9	0/9	0/9
Reject 1976–1978	484	9/9	5/9	5/9	5/9	5/9	8/9
Nonreject 1978–1982	1,116	0/9	0/9	0/9	0/9	0/9	0/9
Reject 1982–1996	3,392	0/9	3/9	2/9	3/9	4/9	8/9
Nonreject 1996–2001	1,325	0/9	1/9	0/9	0/9	0/9	0/9
Reject 2001–2006	1,130	5/9	0/9	0/9	3/9	3/9	7/9
Nonreject 2006–2024	4,761	0/9	0/9	0/9	0/9	0/9	0/9

Notes: Entries report the number of rejected joint zero-alpha tests among the nine body–tail split ratios. The initial partial transition segment in 1967 contains only 169 common-sample observations and is omitted. Regimes are detected from the q5 rolling rejection signal and are used only as a descriptive chronology. HAC standard errors use 21 daily lags.

Rejections concentrate in specific regimes. In the nonreject regimes every model passes at all cutoffs, q5 included, so the partition isolates when the pattern is active rather than labeling q5 a chronic failure. In the 1982–1996 and 2001–2006 reject regimes q5 rejects at 8/9 and 7/9 cutoffs; other models also reject in parts of these periods, but q5 is the most frequent and persistent within each. The 1982–1996 regime is clearest: CAPM never rejects, the Fama–French models reject at 3/9 to 4/9, and q5 at 8/9.

The subperiod results support two conclusions. The body–tail evidence is not a mechanical full-period artifact—it appears across calendar subperiods, 600 rolling windows, and the detected reject regimes, with q5 the most-rejected model in each. And it is time-varying by feature, not defect: strongest from the 1980s to the mid-2000s and weakening recently, switching on and off with the sample period as a mechanical artifact would not. The next section asks which q5 components the active periods load on, treating the time profile as a clue to the mechanism.

7 Robustness and Diagnostics

This section checks the robustness of the body–tail evidence and isolates the factor block behind it. The robustness checks—alternative HAC lags, a cMKT market factor, external

size deciles, and monthly aggregation—establish that the q5 pattern is not an artifact of a particular inference choice, market-factor implementation, test-asset library, or sampling frequency. The factor-block diagnostics—ablations and a loading–premium decomposition—then locate it in q5’s nonmarket profitability–growth block, the same block that Section 4 found to drive q5’s spanning advantage. Unless stated otherwise, daily tables use Newey–West standard errors with 21 daily lags and monthly tables six monthly lags.

7.1 HAC-lag sensitivity

Table 7.1 reports q5 joint zero-alpha p -values for the full-period body–tail test under Newey–West lags of 5, 21, 63, and 252 trading days.

Table 7.1: q5 body–tail joint-test p -values across HAC lags

Split p	NW5	NW21	NW63	NW252
0.500	1.53×10^{-5}	3.30×10^{-5}	5.22×10^{-5}	7.80×10^{-6}
0.600	7.63×10^{-6}	2.57×10^{-5}	5.90×10^{-5}	2.53×10^{-5}
0.750	4.28×10^{-7}	2.40×10^{-6}	3.62×10^{-6}	7.46×10^{-7}
0.800	2.11×10^{-7}	1.21×10^{-6}	1.72×10^{-6}	5.10×10^{-7}
0.850	1.40×10^{-5}	6.25×10^{-5}	8.41×10^{-5}	2.17×10^{-5}
0.900	3.33×10^{-4}	0.001	0.001	8.02×10^{-4}
0.950	0.003	0.007	0.007	0.007
0.975	0.026	0.040	0.035	0.038
0.990	0.004	0.009	0.010	0.018

Notes: The table reports Wald-test p -values for the joint zero-alpha restriction on the body and tail legs. The common daily sample is 1967–2024.

The result is insensitive to this choice: the joint null rejects at all nine ratios under every lag, with the largest p -value across the grid below 0.041. Survival under windows as long as 252 days is also a first piece of evidence against a pure high-frequency-microstructure reading—a pattern generated by daily nonsynchronous trading would not persist through HAC windows of a trading year. The check does not identify the economic source, but removes HAC bandwidth as an explanation.

7.2 Replacing the market factor with cMKT

A direct concern is market-factor mismatch: the q-factor market factor is not exactly my production market return. I therefore replace the native market factor in q5 and FF6 with cMKT, the same return the body and tail legs reconstruct.

Table 7.2: Market-factor replacement and body–tail rejections

Model	Sample	Obs.	Joint reject	Median p_J	$\bar{\alpha}_A$ (bp/yr)	$\bar{\alpha}_B$ (bp/yr)	Sum reject
FF6	1963–2024	15481	0/9	0.567	-10.3	36.7	0/9
cMKT–FF6	1963–2024	15481	1/9	0.425	-9.9	38.3	1/9
q5	1967–2024	14598	9/9	< 0.001	-56.2	181.0	8/9
cMKT–q5	1967–2024	14598	9/9	< 0.001	-50.7	187.7	9/9

Notes: “Joint reject” counts 5% Wald rejections across the nine body–tail split ratios. “Sum reject” counts rejections for $\alpha_A + \alpha_B = 0$. Alphas are annualized basis points. HAC standard errors use 21 daily lags. Net-market p -values for cMKT variants are omitted because the net portfolio is spanned by construction.

The pattern survives replacement: native q5 and cMKT–q5 both reject at all nine cutoffs, with body and tail alphas of similar sign and magnitude. This is the decisive form of the check, because cMKT is the exact return the legs reconstruct and is built from CRSP source data rather than a provider series. If the pattern came from a mismatch between the q5 market factor and the market portfolio being decomposed, aligning the two would remove it; it does not. The source is therefore not the market factor, and the diagnostics below place it in the nonmarket block.

7.3 External size-portfolio diagnostics

The body–tail legs are internal test assets, built from the same universe that reconstructs the market return. I next ask whether the same size-ranked pattern appears in standard external size portfolios: daily value-weighted size deciles from the Kenneth French Data Library and from Open Source Asset Pricing (OSAP), which follows the open-source framework of [Chen and Zimmermann \(2022\)](#). The point is not another battery of test assets but a comparison with familiar size sorts whose construction is independent of my decomposition. I report deciles only; terciles and quintiles are coarser versions of the same French sort, and the decile cut is also the most informative about where the q5 errors sit across the size distribution.

Table 7.3: Daily size-decile joint-alpha tests

Source	Model	p_J	Joint reject	Individual rejects	Mean α (bp/yr)	Median $ \alpha $ (bp/yr)
French	CAPM–FF	0.468	0	0/10	100.1	99.3
French	FF3	0.005	1	3/10	-46.0	39.2
French	Carhart	0.005	1	2/10	-43.6	43.9
French	FF5	0.124	0	1/10	5.2	33.6
French	FF6	0.120	0	1/10	4.1	27.9
French	CAPM–q5	0.469	0	0/10	99.4	98.6
French	q5	9.80×10^{-7}	1	8/10	130.7	146.3
OSAP	CAPM–FF	0.370	0	0/10	86.0	88.5
OSAP	FF3	4.02×10^{-6}	1	4/10	-68.5	106.0
OSAP	Carhart	1.14×10^{-5}	1	4/10	-89.7	79.0
OSAP	FF5	3.46×10^{-4}	1	2/10	18.4	99.3
OSAP	FF6	5.45×10^{-4}	1	2/10	-2.6	90.7
OSAP	CAPM–q5	0.366	0	0/10	84.8	87.7
OSAP	q5	3.05×10^{-4}	1	5/10	180.7	127.3

Notes: The table reports Wald-test p -values for the joint zero-alpha restriction across daily value-weighted size deciles. The sample is January 3, 1967 to December 31, 2024. HAC standard errors use 21 daily lags. “Joint reject” is an indicator for rejection at the 5% level. “Individual rejects” counts single-asset alpha rejections at the 5% level. CAPM–FF uses the Fama–French market factor and risk-free rate. CAPM–q5 uses the q5 market factor and risk-free rate without the nonmarket q5 factors. The OSAP rows use port01–port10; the long–short portfolio is excluded.

Table 7.3 shows construction dependence in the binary rejection but a stable direction underneath it. The rejection itself is library-dependent: in French deciles FF5 and FF6 pass while q5 rejects with eight of ten individual alphas significant, whereas in OSAP deciles FF5, FF6, and q5 all reject, so a pass/fail reading does not isolate q5. The direction of the nonmarket block does. Read against the CAPM–q5 baseline—the q5 market factor and risk-free rate with the nonmarket factors removed—q5 is the only candidate whose nonmarket block *enlarges* the size-decile alpha relative to its own market-only specification: it moves the OSAP mean from 84.8 to 180.7 bp and the French mean from 99.4 to 130.7 bp, while the Fama–French blocks pull the alpha *toward* zero (FF6 takes the OSAP mean from 86.0 to -2.6 bp, and FF5/FF6 sit near 5 bp in French). The rejection is shared in OSAP; the mechanism producing it is not. Because CAPM–q5 itself does not reject in either library, the rejection is a property of the full q5 block, not of the q5 market factor—the same separation the paper documents internally, now in externally constructed portfolios that cross-validate it. French, OSAP, and the body–tail legs are three independent ways to impose a size ranking on U.S. equities: the ranking of q5 against FF5 and FF6 shifts across them, but the direction of the q5 block—adding it widens rather than closes the size-ranked error—does not. Construction

dependence is therefore not a reason to discount the body–tail result but additional evidence that it is a property of the q5 block rather than of any one decomposition.

Table 7.4: q5 alphas across daily size deciles

Decile	French deciles			OSAP deciles		
	α (bp/yr)	$t(\alpha)$	$p(\alpha)$	α (bp/yr)	$t(\alpha)$	$p(\alpha)$
Smallest	231.0	2.26	0.024	481.8	1.98	0.048
D02	0.9	0.01	0.988	410.1	2.09	0.037
D03	109.8	2.28	0.023	413.9	2.75	0.006
D04	81.4	1.75	0.080	164.9	1.53	0.125
D05	174.5	3.41	6.58×10^{-4}	-18.9	-0.25	0.799
D06	179.6	3.14	0.002	40.3	0.76	0.445
D07	251.3	4.48	7.43×10^{-6}	24.1	0.57	0.570
D08	230.1	4.37	1.27×10^{-5}	89.7	2.00	0.045
D09	118.1	2.38	0.018	216.9	4.39	1.12×10^{-5}
Largest	-70.0	-2.98	0.003	-15.7	-1.16	0.244

Notes: The table reports individual q5 alpha estimates for daily value-weighted size deciles. Alphas are annualized basis points. HAC standard errors use 21 daily lags. Deciles are ordered from the smallest to the largest size portfolio within each source. The OSAP long–short portfolio is excluded.

Table 7.4 gives the q5-only cross-section, and it rules out a microcap or nonsynchronous-trading reading. If the pattern were such an artifact, the sharpest alphas should sit at the microcap end; instead they sit in the interior of the size distribution in both libraries—D07 and D08 in French ($t = 4.48, 4.37$), D03 and D09 in OSAP ($t = 2.75, 4.39$)—while the smallest decile is significant in French but only marginal in OSAP ($t = 1.98$). The largest decile carries a negative q5 alpha in both libraries (-70.0 and -15.7 bp), the same sign q5 assigns to the body leg internally. The internal body–tail design agrees: were the pattern a small-stock artifact, it should be sharpest where the tail is most microcap-concentrated, but Table 5.2 shows the q5 tail-alpha t -statistic peaks at 4.37 to 5.14 for split ratios 0.50 to 0.80, where the tail holds 50% to 20% of market value. So the external deciles and the internal decomposition locate the error in the same place—negative large-cap alpha, sharpest positive alphas in the interior—and detailed profiles differ across constructions but that coarse shape does not. Microstructure may move individual estimates but not that location; with the HAC-lag stability of Table 7.1, a pure microstructure reading is hard to sustain.

7.4 Monthly aggregation

I also repeat the body–tail tests after compounding daily returns to calendar months, which reduces the role of daily nonsynchronous trading and short-horizon microstructure. The test uses the same nine split ratios and the common 1967–2024 sample, with Newey–West standard errors at six monthly lags. The monthly sample has 696 observations against 14,598 trading days, so at the same leg-level effect size the joint test has materially lower power: a drift of the p -values toward the margin is what compounding should produce even when the underlying pattern is unchanged.

Table 7.5: Monthly body–tail diagnostics

Model	Joint reject	Sum reject	Median p_J	Median p_S	Body α (bp/yr)	Tail α (bp/yr)
CAPM–FF	0/9	0/9	0.967	0.873	-2.6	7.1
FF3	4/9	4/9	0.170	0.078	20.5	-105.5
Carhart	0/9	0/9	0.635	0.613	7.8	-29.2
FF5	0/9	0/9	0.594	0.324	12.3	-49.9
FF6	0/9	0/9	0.822	0.656	1.9	12.4
CAPM–q5	0/9	0/9	0.924	0.790	-0.5	9.3
q5	1/9	5/9	0.133	0.046	-20.6	116.7

Notes: The table summarizes monthly body–tail pair tests across nine split ratios. The sample contains 696 months from January 1967 to December 2024. Alphas are monthly intercepts multiplied by 12 and reported in annual basis points. p_J is the joint two-leg zero-alpha Wald-test p -value. p_S is the p -value for $\alpha_A + \alpha_B = 0$. HAC standard errors use six monthly lags.

The direction is frequency-invariant; what weakens is significance, not the pattern. The mean body alpha is negative and the mean tail alpha positive in all nine monthly splits, exactly as daily, and the separation of q5 from the others is preserved: CAPM–FF, Carhart, FF5, FF6, and CAPM–q5 reject neither restriction at any ratio (joint median p from 0.59 to 0.97), while q5 is the only model that rejects the alpha-sum restriction—five of nine splits, median alpha-sum p of 0.046—and although its joint median p of 0.133 sits above 5%, it is below every other model by a wide margin. The attenuation is the expected consequence of the twenty-one-fold reduction in nominal sample length: the same effect maps into a smaller t -statistic, so the joint p -value drifts toward the margin without any change in the effect itself.

Table 7.6 confirms that the attenuation is one of significance, not structure. The body alpha is negative and the tail alpha positive at every ratio, the tail-leg t -statistic exceeds two at several ratios (reaching 2.52 at $p = 0.80$, where the joint test rejects outright), and the

strongest evidence again sits in the middle of the grid rather than at $p = 0.99$ where the tail is most microcap-concentrated. The lower frequency moves the p -values toward the margin without disturbing the sign pattern or its cross-sectional location.

Table 7.6: q5 monthly body–tail alphas by split ratio

Split p	Body α (bp/yr)	Tail α (bp/yr)	t_A	t_B	Joint p	$\alpha_A + \alpha_B$ (bp/yr)	Sum p
0.500	-51.5	52.7	-1.38	1.46	0.325	1.2	0.862
0.600	-45.3	70.3	-1.57	1.71	0.200	25.0	0.074
0.750	-26.4	83.1	-1.73	1.99	0.119	56.6	0.040
0.800	-26.2	109.2	-2.14	2.52	0.034	83.0	0.010
0.850	-13.8	83.8	-1.53	1.95	0.130	70.0	0.046
0.900	-10.1	98.3	-1.47	2.06	0.106	88.2	0.036
0.950	-6.2	129.9	-1.25	1.91	0.161	123.6	0.056
0.975	-3.7	158.3	-0.90	1.64	0.262	154.6	0.102
0.990	-2.6	265.1	-0.73	2.01	0.133	262.5	0.045

Notes: This table reports q5 body–tail results after compounding daily portfolio returns to calendar months. The sample contains 696 months from January 1967 to December 2024. A denotes the body leg and B denotes the tail leg. Alphas are monthly intercepts multiplied by 12 and reported in annual basis points. Newey–West standard errors use six monthly lags.

The frequency result does not undercut the daily evidence, because the daily q5 factors are not a construction of mine but the series the providers distribute at the daily frequency ([Global-q.org](https://global-q.org), 2026); the stronger daily rejection therefore cannot be dismissed as an artifact of converting a monthly model to daily data. The attenuation is consistent with averaging of the daily leg covariance structure, not with daily measurement error—pure daily noise would not retain the same sign in all nine monthly splits. The CAPM–q5 versus q5 contrast also recurs: the q5 market factor and risk-free rate alone pass the monthly test while the full q5 block produces the body-negative, tail-positive pattern, reinforcing the market-factor replacement result and setting up the factor-block diagnostics that follow.

7.5 Factor-block ablation across model families

Table 7.7 summarizes selected ablations—a within-family diagnostic, not a sample-controlled horse race—showing how the body–tail pattern changes when specific factor blocks are removed or restricted.

Table 7.7: Selected factor-block ablations across model families

Family	Variant	Kept factors	Sample	Joint reject	Median p_J	$\bar{\alpha}_A$ (bp/yr)	$\bar{\alpha}_B$ (bp/yr)
FF3	Full FF3	MKT+SMB+HML	1926–2024	1/9	0.230	12.6	-7.6
	MKT only	MKT	1926–2024	2/9	0.103	-22.0	164.1
	Drop SMB	MKT+HML	1926–2024	1/9	0.328	-8.5	101.3
	Drop HML	MKT+SMB	1926–2024	1/9	0.273	-2.9	65.4
Carhart	Full Carhart	MKT+SMB+HML+UMD	1926–2024	1/9	0.384	4.3	40.8
	MKT only	MKT	1926–2024	2/9	0.092	-23.3	168.6
	Drop HML	MKT+SMB+UMD	1926–2024	8/9	0.019	-15.0	130.7
	Drop UMD	MKT+SMB+HML	1926–2024	1/9	0.257	11.9	-6.4
FF5	Full FF5	MKT+SMB+HML+RMW+CMA	1963–2024	0/9	0.745	-2.3	-14.4
	MKT only	MKT	1963–2024	0/9	0.667	-21.2	98.4
	Drop SMB	MKT+HML+RMW+CMA	1963–2024	2/9	0.086	-48.3	222.0
	Drop RMW	MKT+SMB+HML+CMA	1963–2024	3/9	0.450	10.4	-61.6
FF6	Full FF6	MKT+SMB+HML+RMW+CMA+UMD	1963–2024	0/9	0.567	-10.3	36.7
	MKT only	MKT	1963–2024	0/9	0.667	-21.2	98.4
	Drop SMB	MKT+HML+RMW+CMA+UMD	1963–2024	7/9	0.030	-55.8	270.6
	Drop UMD	MKT+SMB+HML+RMW+CMA	1963–2024	0/9	0.745	-2.3	-14.4
q5	Full q5	MKT+ME+IA+ROE+EG	1967–2024	9/9	< 0.001	-56.2	181.0
	MKT only	MKT	1967–2024	0/9	0.768	-18.9	81.5
	Drop EG	MKT+ME+IA+ROE	1967–2024	2/9	0.098	-26.8	106.6
	Drop ROE	MKT+ME+IA+EG	1967–2024	6/9	0.001	-51.0	151.8
	Drop ME	MKT+IA+ROE+EG	1967–2024	9/9	< 0.001	-143.7	629.1

Notes: “Joint reject” counts 5% Wald rejections across the nine body–tail split ratios. HAC standard errors use 21 daily lags.

The traditional Fama–French specifications are broadly stable. Removing SMB from FF5 or FF6 raises body–tail rejections, so the size block absorbs part of the size-ranked decomposition rather than generating it: size enters on the stabilizing side. q5 behaves oppositely. Its market-only variant rejects at no cutoff while the full specification rejects at all nine, so adding the q5 nonmarket block turns a passing decomposition into a rejected one—the same direction seen in the external size deciles.

Within the q5 block, the rejections track the profitability–growth side rather than size. Dropping EG collapses the pattern from 9/9 to 2/9 (median $p_J = 0.098$) and dropping ROE leaves more in place at 6/9, so EG carries most of the effect and ROE the remainder; dropping ME, by contrast, not only keeps all nine rejections but amplifies the leg alphas (to -143.7 and 629.1 bp), confirming once more that the source is not a missing size factor. The next subsection decomposes this block.

7.6 The ROE–EG block in q5

Table 7.8 examines q5 variants more closely. With the native market factor (Panel A), MKT-only, MKT+ME, and MKT+ME+IA produce no joint rejections; rejections appear

only once ROE or EG enters, and the attenuation is largest when EG is removed—dropping EG cuts rejections from nine to two while dropping ROE leaves six—so EG carries most of the body–tail sensitivity, ROE second. This is the point of contact with Section 4, where EG was the single largest contributor to q5’s mean–variance advantage over FF6, with an individual ΔSR^2 of 2.425: the factor that most expands the q5 opportunity set is the one most associated with the body–tail pricing error. The sensitivity is also specific to the q-family profitability construction, not to profitability factors in general—with expected growth absent, MKT+ME+ROE rejects at three ratios while MKT+ME+RMW rejects at none, and replacing ROE with the Fama–French RMW does not remove the pattern when EG remains. Panel B repeats the diagnostic with cMKT-based variants and reaches the same ranking, so it does not depend on the market factor. I read these comparisons as evidence about which block carries the pattern in this design, not that any factor is economically invalid.

Table 7.8: q5 factor-block diagnostics

Variant	Kept factors	Joint reject	Median p_J	$\bar{\alpha}_A$ (bp/yr)	$\bar{\alpha}_B$ (bp/yr)	Sum reject
<i>Panel A: Native q5 market factor</i>						
Full q5	MKT+ME+IA+ROE+EG	9/9	< 0.001	-56.2	181.0	8/9
MKT only	MKT	0/9	0.768	-18.9	81.5	0/9
MKT+ME	MKT+ME	0/9	0.530	12.9	-77.3	4/9
MKT+ME+IA	MKT+ME+IA	0/9	0.429	11.2	-72.1	3/9
MKT+ME+ROE	MKT+ME+ROE	3/9	0.094	-27.0	110.1	4/9
MKT+ME+EG	MKT+ME+EG	6/9	0.008	-48.8	144.7	6/9
MKT+ME+RMW	MKT+ME+RMW	0/9	0.809	-3.7	-15.7	0/9
Drop EG	MKT+ME+IA+ROE	2/9	0.098	-26.8	106.6	5/9
Drop ROE	MKT+ME+IA+EG	6/9	0.001	-51.0	151.8	6/9
ROE to RMW	MKT+ME+IA+RMW+EG	8/9	< 0.001	-53.5	161.4	7/9
<i>Panel B: Production market return (cMKT)</i>						
Full cMKT q5	cMKT+ME+IA+ROE+EG	9/9	< 0.001	-50.7	187.7	9/9
cMKT+ME+IA	cMKT+ME+IA	1/9	0.247	11.6	-70.6	2/9
cMKT+ME+EG	cMKT+ME+EG	7/9	0.002	-44.2	150.2	7/9
cMKT+ME+RMW	cMKT+ME+RMW	1/9	0.591	-2.2	-13.3	0/9
ROE to RMW	cMKT+ME+IA+RMW+EG	8/9	< 0.001	-47.9	168.3	8/9

Notes: q5 ablations over 1967–2024. “Joint reject” and “Sum reject” count 5% rejections across the nine body–tail split ratios; alphas are annualized basis points; HAC standard errors use 21 daily lags. Panel A uses the native q5 market factor. Panel B replaces it with the production market return cMKT, for which net-alpha p -values are omitted because the net market is mechanically spanned by cMKT.

The ablations therefore place the body–tail sensitivity in the q5 profitability–growth block. ME stabilizes the decomposition—dropping it strengthens the rejection and sharply raises the tail alpha—while the pattern is most pronounced when ROE and EG are present,

and the cMKT panel gives the same ranking, ruling out the market factor as the driver. The interpretation is deliberately narrow: the ablations identify the block associated with the pricing-error pattern in this design, not that the factors are misspecified in a mean–variance sense, where Section 4 showed the same block is q5’s main strength. That a single block is the source of both the spanning advantage and the body–tail pricing error is precisely the separation between the two criteria that motivates the paper.

7.7 Loading–premium decomposition

The ablations show where to look; I next decompose the tail-minus-body spread. For each split, let $\hat{c}_k = (\hat{\beta}_{T,k} - \hat{\beta}_{B,k}) \bar{f}_k$, so the average tail-minus-body spread splits into an alpha spread and a factor-implied spread,

$$\bar{R}_T - \bar{R}_B = \hat{\alpha}_{T-B} + \sum_k \hat{c}_k,$$

with all nine pairs reconstructing the production market numerically and all identity checks passing.

Table 7.9: q5 loading–premium decomposition of tail-minus-body spreads

Model	Window	Actual (bp/yr)	Factor (bp/yr)	Alpha (bp/yr)	MKT (bp/yr)	ME (bp/yr)	IA (bp/yr)	ROE (bp/yr)	EG (bp/yr)
q5	Full period	88.3	-148.9	237.2	-28.0	170.9	0.9	-166.5	-126.2
cMKT–q5	Full period	88.3	-150.1	238.4	-28.6	170.9	0.7	-166.4	-126.6
q5	Rolling 5y	76.6	-148.8	225.4	-32.2	147.1	15.7	-139.1	-140.2
cMKT–q5	Rolling 5y	76.6	-149.4	226.0	-32.5	147.0	15.3	-139.0	-140.1

Notes: The table averages across the nine split ratios. “Actual” is the realized tail-minus-body spread. “Factor” is the sum of factor-loading contributions. “Alpha” is Actual minus Factor. Rolling 5y rows average over all rolling five-year windows and split ratios.

The sign pattern is the main diagnostic result. The realized tail-minus-body spread is positive (88.3 bp) while the q5 factor-implied spread is negative (–148.9 bp), leaving a large positive residual alpha spread (237.2 bp). The components show why: ME contributes positively (170.9 bp), consistent with the small-stock exposure of the tail, but ROE and EG contribute negatively (–166.5 and –126.2 bp) and more than offset it. The factor-implied spread is negative not despite the size block but against it—the profitability–growth block pulls the implied tail return below the body, while the realized tail return is above it.

Table 7.10: Sign persistence in rolling five-year windows

Model	Observations	$\Pr(\alpha_{T-B} > 0)$ (%)	$\Pr(c_{ME} > 0)$ (%)	$\Pr(c_{ROE} < 0)$ (%)	$\Pr(c_{EG} < 0)$ (%)
q5	5733	84.8	58.7	96.2	90.7
cMKT-q5	5733	84.8	58.7	96.2	90.7

Notes: Observations are rolling five-year window by split-ratio pairs. There are 637 windows and nine split ratios for each model.

The structure persists in rolling windows: the alpha spread is positive in about 85% of split-window observations, and the ROE and EG contributions are negative in most (96.2% and 90.7%). The full-sample decomposition is thus not the product of one period or one split ratio, and it fixes the time-variation result of Section 6—the pattern is active when the negative ROE and EG contributions are large, the same channel through which the rejection switches on and off across decades.

Table 7.11: Nonoverlapping phase regressions for alpha spreads

Model	Regressor	Phases	Positive slope (%)	Median R^2	Median corr.	Significant (%)
q5	c_{ME}	60	86.7	0.147	0.384	78.3
q5	c_{IA}	60	53.3	0.043	0.032	58.3
q5	$-c_{ROE}$	60	96.7	0.048	0.218	55.0
q5	$-c_{EG}$	60	98.3	0.095	0.309	78.3
cMKT-q5	c_{ME}	60	86.7	0.147	0.383	76.7
cMKT-q5	c_{IA}	60	53.3	0.043	0.030	56.7
cMKT-q5	$-c_{ROE}$	60	96.7	0.047	0.218	55.0
cMKT-q5	$-c_{EG}$	60	98.3	0.093	0.306	76.7

Notes: Each phase uses nonoverlapping five-year windows. The dependent variable is the alpha spread across split ratios within a phase. “Significant” is the share of phases with a 5% significant slope. Regressors with a minus sign are multiplied by -1 so that a positive slope means a larger negative contribution is associated with a larger alpha spread.

Nonoverlapping phases give the same message without the overlapping-window concern: larger negative EG and ROE contributions are associated with larger alpha spreads in 98.3% and 96.7% of phases.

Table 7.12: Rolling-window HAC regressions of alpha spreads on factor contributions

Model	c_{ME}	c_{IA}	c_{ROE}	c_{EG}	R^2
q5	0.253*** (4.20)	-0.475 (-1.10)	-0.945*** (-6.06)	-0.292** (-2.46)	0.543
cMKT–q5	0.253*** (4.21)	-0.462 (-1.07)	-0.949*** (-6.05)	-0.283** (-2.38)	0.543

Notes: The dependent variable is the rolling five-year alpha spread averaged across split ratios. Coefficients are reported with Newey–West t -statistics in parentheses. The HAC lag is 60 months. *, **, and *** denote 10%, 5%, and 1% significance.

The regression confirms the decomposition: alpha spreads are larger when the ROE and EG contributions are more negative, while ME enters with the opposite sign. The evidence therefore does not support a missing-size-factor reading—in this design the size block contributes on the stabilizing side, and the ROE–EG block is the source of the negative q5 factor-implied tail-minus-body spread that the positive realized spread must overcome. This is the mechanism behind the headline pattern: q5 assigns the size-ranked tail too low a factor-implied return—because the tail loads on ROE and EG in a way that, at the q5 premia, implies a lower return than the body—so a positive realized tail-minus-body spread is left as a positive alpha spread. The conclusion is diagnostic and design-specific: it describes how q5 allocates factor-implied returns across this size-ranked decomposition, not a general failure of the profitability or expected-growth factors, which on the spanning criterion are q5’s strongest components.

8 Discussion

8.1 What the diagnostic adds, and its relation to spanning

The aggregate market regression is a useful sanity check but a weak place to stop when the model already contains a market factor. The body–tail diagnostic keeps that aggregate relation intact and asks a different question: once the same CRSP investible universe is decomposed into tradable size-ranked legs, do pricing errors remain hidden inside the market portfolio?

For q5 the answer is yes. The production market return has a small, insignificant alpha under every model, yet once the market is split by cumulative market capitalization q5 leaves a repeated negative-body, positive-tail pattern that the other five do not. Because the legs dynamically recombine to the aggregate market, this is not a test of whether the market identity holds but of whether a model that prices the aggregate also prices its internal

components; and since the recombination identity holds for every model alike, only q5 leaving the pattern cannot be a mechanical consequence of the split. The random splits confirm this—removing only the size ranking, the matched placebo rejects at 4.1% for q5, close to nominal, against rejection at all nine deterministic cutoffs. This is the main empirical contribution: a low-dimensional model can fit an aggregate portfolio while leaving pricing errors on portfolios formed from the same universe, made visible by holding the aggregate benchmark, the universe, the formation dates, and the recombination fixed, so the only substantive design choice is the size-ranked assignment rule.

The contribution sits against the two criteria of Section 2.1, which coincide for an ideal SDF but come apart for an approximation. On the spanning criterion of Barillas and Shanken (2017) and Barillas and Shanken (2018), which governs model comparison, q5 is the strongest candidate: its ROE and expected-growth factors expand the mean–variance frontier well beyond FF6. On a size-ranked decomposition of the very market it prices in aggregate, the same model leaves systematic, opposite-signed leg alphas. These are not in tension; they are two sides of an approximate SDF. The body–tail diagnostic does not rank models through test-asset alphas, so it does not contradict the test-asset-irrelevance result, which concerns model *comparison*: it asks a within-model question, whether a model prices an economically ordered decomposition of its own market portfolio, and the answer can differ from the model’s mean–variance standing. The sharpest form is that one factor block produces both outcomes—expected growth is the single largest contributor to q5’s spanning advantage and the factor whose removal most attenuates the body–tail pattern. A factor can expand the investment opportunity set and, through the same loadings and premia, misprice a particular set of portfolios—the separation the paper documents, made concrete in one model.

8.2 Locating the source, and what it is not

The diagnostics locate the pattern on the nonmarket side of q5. It is not a market-factor issue: CAPM with the q5 market factor passes the body–tail and external size checks far more cleanly than full q5, and substituting the production market return cMKT does not remove it. Within the block, MKT+ME and MKT+ME+IA are stable while rejections appear once the profitability–growth factors enter—dropping EG attenuates most, dropping ROE leaves more in place, and replacing ROE with RMW does not remove it while EG remains.

The loading–premium decomposition explains the sign. The realized tail-minus-body spread is positive but the q5 factor-implied spread is negative, so the residual alpha spread is positive, with ME contributing in the expected direction for a small-stock tail but ROE

and EG moving the other way and dominating. This is not a missing-size-factor story—the size block stabilizes the spread and the profitability–growth block reverses it: the full q5 block assigns the size-ranked tail too low a factor-implied return relative to the body, generating the opposite-signed leg alphas even though the aggregate benchmark is passed.

The same direction appears in externally constructed size portfolios, so the result is not specific to my decomposition. In French deciles FF5 and FF6 pass the joint-alpha test while q5 rejects; in OSAP deciles FF5, FF6, and q5 all reject, so the binary outcome does not isolate q5—but the direction does. Relative to its market-only baseline (CAPM–q5), q5 is the only candidate whose nonmarket factors *enlarge* the mean decile alpha in both libraries, while the Fama–French blocks pull theirs toward zero. French deciles, OSAP deciles, and the body–tail legs are different size-ranked test assets on which the *ranking* of q5 against FF5 and FF6 shifts but the *direction* does not, and the body–tail design is the most controlled version because its legs recombine exactly to the production market portfolio.

The pattern is also not a microstructure or low-frequency artifact. Were it driven by microcaps or nonsynchronous trading, the sharpest evidence should sit in the smallest portfolios; instead the q5 tail alphas are sharp even when the tail is a large share of market value, the smallest OSAP decile is insignificant, and the largest French q5 *t*-statistics fall in the middle and upper-middle deciles. Nor does lower frequency dissolve it: under monthly aggregation the sign pattern survives in all nine splits and q5 remains the only model rejecting the alpha-sum restriction, though the joint evidence weakens. The defensible claim is not that q5 fails every size-ranked test at every frequency, but that the full q5 block produces a residual pattern surviving changes in inference, market factor, test-asset library, and frequency, absent from its own market-only benchmark—and since the daily q5 factors are the providers’ published series, not a frequency conversion of mine, the monthly attenuation does not weaken the daily evidence.

8.3 Scope, time variation, and the choice of axis

The pattern is not constant over time, and its variation tracks the mechanism. Rolling and regime diagnostics show strong rejections from the 1980s through the mid-2000s and weak evidence recently; the loading–premium regressions show the alpha spread is larger when the ROE and EG contributions are more negative, so as those premia weaken the negative factor-implied spread loses force and the rejection attenuates—switching on and off with the sample period as a factor-block mechanism would, not as a fixed artifact would. This is descriptive, not a causal claim: body–tail alpha depends on factor means, leg loadings, and covariances jointly, so a weaker EG premium is consistent with weaker recent rejections

without being the sole cause. It also sharpens interpretation—the diagnostic does not label q5 a chronic failure, since q5 passes at every cutoff in the nonreject regimes, but identifies when the profitability–growth block prices the size-ranked decomposition strongly.

The evidence is otherwise specific to an investible CRSP common-stock portfolio and to cumulative-market-cap decompositions. The universe filters, delisting and reinvestment treatment, annual formation, and HAC choices are part of the design, and the robustness tests reduce the concern that the result is mechanical without implying invariance across every market definition. That French and OSAP deciles do not give identical rankings reinforces this—not a weakness but evidence that evaluation is sensitive to test-asset construction—and the body–tail decomposition is useful precisely because it makes one construction transparent and anchors it to the aggregate market return.

Cumulative market capitalization is the natural axis for three reasons already in the analysis. First, the theory points to it: by [Kozak et al. \(2018\)](#), an approximate SDF is carried by a few high-variance covariance directions, of which size is the leading one in U.S. equities, so a size-ranked decomposition loads on where the approximation is most consequential rather than on an arbitrary characteristic. Second, it preserves the aggregate-market identity: cutting by cumulative market capitalization lets the value-weighted recombination reconstruct the production market return exactly, holding the benchmark fixed in a way a non-size split would weaken. Third, the mechanism selects it *ex post*: the loading–premium decomposition shows the q5 profitability–growth block imposes a return gradient aligned with the size cross-section, so the size cut is diagnostically informative rather than a partition chosen because it happened to reject. Other economically ordered decompositions are possible, and I leave them to future work—the point is not that size is the only informative cut, but that it is the one for which the aggregate relation is exactly preserved and the mechanism identified. Passing an aggregate market sanity check thus does not guarantee pricing consistency across market-derived test assets: aggregate market fit, mean–variance spanning, and the alpha pattern on a size-ranked decomposition are three distinct empirical objects, and a model can stand differently on each.

9 Conclusion

I study whether a factor model that prices the aggregate market also prices size-ranked portfolios formed from the same universe. The aggregate regression is a useful but limited check when the model already contains a market factor, so I split an investible CRSP market portfolio into body and tail legs by cumulative market capitalization—tradable portfolios whose dynamic value-weighted recombination reconstructs the aggregate market return, holding

that relation fixed while asking whether pricing errors appear inside the market.

The aggregate portfolio has small alphas and very high explanatory power under all six models, but the decomposition separates them: in the full daily sample q5 rejects the joint zero-alpha restriction at all nine split ratios, with negative body and positive tail alpha, while CAPM, Carhart, FF5, and FF6 are stable. Because the recombination identity holds for every model, this difference cannot be mechanical, and the opposite-signed leg pattern is hidden by the aggregate regression all six pass. Matched random splits, alternative HAC lags, the cMKT substitution, external French and OSAP size deciles, and monthly aggregation leave the pattern and the separation of q5 intact, while factor-block ablations and a loading–premium decomposition place it in the nonmarket profitability–growth block rather than a missing size factor.

The conclusion is not that q5 is dominated under every criterion. On the spanning criterion of [Barillas and Shanken \(2017\)](#), which governs model comparison, q5 is the strongest candidate, its ROE and expected-growth factors expanding the mean–variance frontier well beyond FF6; on a size-ranked decomposition of the market it prices in aggregate, the same model leaves systematic, opposite-signed alphas. The sharpest expression is a single factor: expected growth is both the largest contributor to q5’s spanning advantage and the factor whose removal most attenuates the body–tail pattern. Aggregate market fit, mean–variance spanning, and the alpha pattern on an economically interpretable decomposition are thus three distinct objects, and a model can stand differently on each—passing the market regression does not rule out systematic alphas inside the same universe, and spanning strength does not guarantee them away. The body–tail diagnostic provides a simple way to hold the aggregate relation fixed and make that distinction visible.

Funding This research did not receive any specific grant from funding agencies in the public, commercial, or not-for-profit sectors.

Declaration of AI usage During the preparation of this manuscript, the author used ChatGPT (OpenAI) and Claude (Anthropic) for language refinement and structural clarity. All outputs were reviewed and edited by the author, who takes full responsibility for the content.

Declaration of interest The author declares no competing interests.

References

- Gibbons, M. R., Ross, S. A., & Shanken, J. (1989). A test of the efficiency of a given portfolio. *Econometrica*, 57(5), 1121–1152. <https://www.jstor.org/stable/1913625>
- Lo, A. W., & MacKinlay, A. C. (1990). Data-snooping biases in tests of financial asset pricing models. *The Review of Financial Studies*, 3(3), 431–467. <https://doi.org/10.1093/rfs/3.3.431>
- Hansen, L. P., & Jagannathan, R. (1997). Assessing specification errors in stochastic discount factor models. *The Journal of Finance*, 52(2), 557–590. <https://doi.org/10.1111/j.1540-6261.1997.tb04813.x>
- Cochrane, J. H. (2005). *Asset Pricing* (Revised ed.). Princeton University Press. <https://www.johnhcochrane.com/asset-pricing>
- Lewellen, J., Nagel, S., & Shanken, J. (2010). A skeptical appraisal of asset-pricing tests. *Journal of Financial Economics*, 96(2), 175–194. <https://doi.org/10.1016/j.jfineco.2009.09.001>
- Barillas, F., & Shanken, J. (2017). Which alpha? *The Review of Financial Studies*, 30(4), 1316–1338. <https://doi.org/10.1093/rfs/hhw101>
- Barillas, F., & Shanken, J. (2018). Comparing asset pricing models. *The Journal of Finance*, 73(2), 715–754. <https://doi.org/10.1111/jofi.12607>
- Kozak, S., Nagel, S., & Santosh, S. (2018). Interpreting factor models. *The Journal of Finance*, 73(3), 1183–1223. <https://doi.org/10.1111/jofi.12612>
- Chen, A. Y., & Zimmermann, T. (2022). Open source cross-sectional asset pricing. *Critical Finance Review*, 11(2), 207–264. <https://doi.org/10.1561/104.00000112>
- Giglio, S., Xiu, D., & Zhang, D. (2025). Test assets and weak factors. *The Journal of Finance*, 80(1), 259–319. <https://doi.org/10.1111/jofi.13415>
- Shin, U. (2026). Which portfolios? The construction dependence of factor model performance. *arXiv preprint arXiv:2606.19550*. <https://doi.org/10.48550/arXiv.2606.19550>
- Jegadeesh, N., & Titman, S. (1993). Returns to buying winners and selling losers: Implications for stock market efficiency. *The Journal of Finance*, 48(1), 65–91. <https://doi.org/10.1111/j.1540-6261.1993.tb04702.x>
- Carhart, M. M. (1997). On persistence in mutual fund performance. *The Journal of Finance*, 52(1), 57–82. <https://doi.org/10.1111/j.1540-6261.1997.tb03808.x>
- Fama, E. F., & French, K. R. (1992). The cross-section of expected stock returns. *The Journal of Finance*, 47(2), 427–465. <https://doi.org/10.1111/j.1540-6261.1992.tb04398.x>

- Fama, E. F., & French, K. R. (1993). Common risk factors in the returns on stocks and bonds. *Journal of Financial Economics*, 33(1), 3–56. [https://doi.org/10.1016/0304-405X\(93\)90023-5](https://doi.org/10.1016/0304-405X(93)90023-5)
- Fama, E. F., & French, K. R. (2015). A five-factor asset pricing model. *Journal of Financial Economics*, 116(1), 1–22. <https://doi.org/10.1016/j.jfineco.2014.10.010>
- Fama, E. F., & French, K. R. (2018). Choosing factors. *Journal of Financial Economics*, 128(2), 234–252. <https://doi.org/10.1016/j.jfineco.2018.02.012>
- Hou, K., Xue, C., & Zhang, L. (2015). Digesting anomalies: An investment approach. *The Review of Financial Studies*, 28(3), 650–705. <https://doi.org/10.1093/rfs/hhu068>
- Hou, K., Mo, H., Xue, C., & Zhang, L. (2019). Which factors? *Review of Finance*, 23(1), 1–35. <https://doi.org/10.1093/rof/rfy032>
- Hou, K., Xue, C., & Zhang, L. (2020). Replicating anomalies. *The Review of Financial Studies*, 33(5), 2019–2133. <https://doi.org/10.1093/rfs/hhy131>
- Hou, K., Mo, H., Xue, C., & Zhang, L. (2021). An augmented q-factor model with expected growth. *Review of Finance*, 25(1), 1–41. <https://doi.org/10.1093/rof/rfaa004>
- Hou, K., Mo, H., Xue, C., & Zhang, L. (2024). The economics of security analysis. *Management Science*, 70(1), 164–186. <https://doi.org/10.1287/mnsc.2022.4640>
- Center for Research in Security Prices, LLC. (2026). *CRSP US Stock Databases* [Data set]. Accessed via Wharton Research Data Services, June 5, 2026. <https://www.crsp.org/research/>
- French, K. R. (2026). *Kenneth R. French Data Library* [Data set]. Accessed May 5, 2026. https://mba.tuck.dartmouth.edu/pages/faculty/ken.french/data_library.html
- Global-q.org. (2026). *Factors and testing portfolios* [Data set]. Accessed May 5, 2026. <https://global-q.org/factors.html>
- Open Source Asset Pricing. (2026). *Open Source Asset Pricing* [Data set]. Accessed June 24, 2026. <https://www.openassetpricing.com>